
PLATO: Policy Learning using Adaptive Trajectory Optimization

Gregory Kahn*, Tianhao Zhang*, Sergey Levine†, Pieter Abbeel*

*University of California, Berkeley, Department of Electrical Engineering and Computer Sciences

†University of Washington, Department of Computer Science and Engineering

Abstract

Policy search can in principle acquire complex strategies for control of robots and other autonomous systems. When the policy is trained to process raw sensory inputs, such as images and depth maps, it can acquire a strategy that combines perception and control. However, effectively processing such complex inputs requires an expressive policy class, such as a large neural network. These high-dimensional policies are difficult to train, especially when training must be done for safety-critical systems. We propose PLATO, an algorithm that trains complex control policies with supervised learning, using model-predictive control (MPC) to generate the supervision. PLATO uses an adaptive training method to modify the behavior of MPC to gradually match the learned policy, in order to generate training samples at states that are likely to be visited by the policy while avoiding highly undesirable on-policy actions. We prove that this type of adaptive MPC expert produces supervision that leads to good long-horizon performance of the resulting policy. We also empirically demonstrate that MPC can still avoid dangerous on-policy actions in unexpected situations during training. Our empirical results on a set of challenging simulated aerial vehicle tasks demonstrate that, compared to prior methods, PLATO learns faster, experiences substantially fewer catastrophic failures (crashes) during training, and often converges to a better policy.

1 Introduction

Policy search via optimization or reinforcement learning (RL) holds the promise of automating a wide range of decision making and control tasks, in domains ranging from robotic manipulation to self-driving vehicles. One particularly appealing prospect is to use policy search techniques to automatically acquire policies that subsume perception and control, thereby acquiring end-to-end perception-control systems that are adapted to the task.

However, representing policies that combine perception and control requires either a careful choice of features or the use of rich and expressive function approximators. Recent results in perception domains, such as computer vision, natural language processing, and speech recognition, suggest that large, expressive function approximators, such as neural networks, can outperform hand-designed features when trained directly on raw input data [8] while requiring substantially less manual engineering. Recent years have seen considerable research on using deep networks for control tasks, including playing Atari games [16], navigation for mobile robots [3], autonomous driving [1], robotic manipulation from camera images [12], and other tasks [13, 5, 22].

Unfortunately, training such large, high-dimensional policies on real physical systems is exceedingly challenging for two reasons. First, standard model-free reinforcement learning algorithms are difficult to apply to large non-linear function approximators [2]. Several recent methods demonstrate RL-based training of large neural networks [16, 22, 13, 5], but these approaches require a very large amount of experience, making them difficult to run on physical systems. In contrast, methods based

on supervised learning, including DAgger [20], guided policy search [11, 12] and the work presented in this paper, are more sample-efficient, but require a viable source of supervision. The second obstacle to using RL in the real world is that, although a fully trained neural network controller can be very robust and reliable, a partially trained policy can perform unreasonable and even unsafe actions [20]. This can be a major problem when the agent is a mobile robot or autonomous vehicle and unsafe actions can cause the destruction of the robot or damage to its surroundings.

We propose PLATO (Policy Learning using Adaptive Trajectory Optimization), a method for training complex policies that combine perception and control by using a trajectory optimization teacher in the form of model-predictive control (MPC). At training time, MPC chooses actions that make a tradeoff between succeeding at the task and matching the behavior of the current policy. By gradually adapting to the policy, MPC ensures that the states visited during training will allow the policy to learn good long-horizon performance. MPC makes use of full state information, which could be obtained, for example, by instrumenting the environment at training time. The final policy, however, is trained to mimic the MPC actions using only the observations available to the robot, which makes it possible to run the resulting policy at test time without any instrumentation. The algorithm requires access to at least a rough model of the system dynamics in order to run MPC during training, but does not require any knowledge of the observation model, making it feasible to use with complex, raw observation signals, such as images and depth scans. Since MPC is used to select all actions at training time, the algorithm never requires running a partially trained and potentially unsafe policy.

We prove that the policy learned by PLATO converges to a policy with bounded cost. Our empirical results further demonstrate that PLATO can learn complex policies for simulated quadrotor flight with laser rangefinder observations and camera observations in cluttered environments and at high speeds. We show that PLATO outperforms a number of previous approaches in terms of both the performance of the final neural network policy and the robustness to catastrophic failure during training. In comparisons with MPC-guided policy search [25], the DAgger algorithm [20], DAgger with coaching [4] and supervised learning, our approach experiences substantially fewer catastrophic failures both during training time and at test time.

2 Preliminaries and Overview

We address the problem of learning control policies for dynamical systems, such as robots and autonomous vehicles. The system is defined by states \mathbf{x} and actions \mathbf{u} . The policy must control the system from observations \mathbf{o} , which are in general insufficient for determining the full state \mathbf{x} . The policy is a conditional distribution over actions $\pi_\theta(\mathbf{u}|\mathbf{o}_t)$, parameterized by θ . At test time, the agent chooses actions according to $\pi_\theta(\mathbf{u}|\mathbf{o}_t)$ at each time step t , and experiences a loss $c(\mathbf{x}_t, \mathbf{u}_t)$. We assume without loss of generality that $c(\mathbf{x}_t, \mathbf{u}_t)$ is in the interval $[0, 1]$. The agent is then taken to the next state according to the dynamics $p(\mathbf{x}_{t+1}|\mathbf{x}_t, \mathbf{u}_t)$. The goal is to learn a policy $\pi_\theta(\mathbf{u}|\mathbf{o}_t)$ that minimizes the total expected cost $J(\pi) = E_\pi[\sum_{t=1}^T c(\mathbf{x}_t, \mathbf{u}_t)]$. We will use $J_t(\pi|\mathbf{x}_t) = E_\pi[\sum_{t'=t}^T c(\mathbf{x}_{t'}, \mathbf{u}_{t'})|\mathbf{x}_t]$ as shorthand for the expected cost starting from state \mathbf{x}_t at time t , such that $J(\pi) = E_{\mathbf{x}_1 \sim p(\mathbf{x}_1)}[J_1(\pi|\mathbf{x}_1)]$, where $p(\mathbf{x}_1)$ is the initial state distribution.

In this work, we further assume that during training, our algorithm has access to the true underlying states \mathbf{x} . This additional assumption allows us to use simple and efficient model-predictive control (MPC) methods to generate training actions. We do not require knowing the true states \mathbf{x} at test time, since the learned policy $\pi_\theta(\mathbf{u}|\mathbf{o}_t)$ only requires observations. This type of training setup could be implemented in various ways in practice, including instrumenting the training environment (e.g. using motion capture to track a mobile robot) or using more effective hardware at training time (such as a more accurate GPS system), while substituting cheaper and more practical hardware at test time. While this additional assumption does introduce some restrictions, we will show that it enables very efficient and relatively safe training, making it an appealing option for safety-critical systems.

We will train the policy $\pi_\theta(\mathbf{u}|\mathbf{o}_t)$ by mimicking a computational “teacher,” rather than attempting to learn the policy directly with reinforcement learning. There are three key advantages to this approach: first, the teacher can exploit the true state \mathbf{x} , while the final policy π_θ is only trained on the observations \mathbf{o} ; second, we can choose a teacher that will remain safe and stable, avoiding dangerous actions during training; third, we can train the final policy π_θ using standard, robust supervised learning algorithms, which will allow us to construct a simple and highly data-efficient algorithm that scales easily to complex, high-dimensional policy parameterizations. Specifically, we will use MPC

as the teacher. MPC uses the true state \mathbf{x} and a model of the system dynamics (which we assume to be known in advance, but which in general could also be learned from experience). MPC plans locally optimal trajectories with respect to the dynamics, and by replanning every time step, is able to achieve considerable robustness to unexpected perturbations and model errors [15], making it an excellent choice for sample-efficient learning.

3 Policy Learning using Adaptive Trajectory Optimization

One naïve approach to learn a policy from a computational teacher such as MPC would be to generate a training set with MPC, and then train the policy with supervised learning to maximize the log-likelihood of this dataset. The teacher can safely choose robust, near-optimal trajectories. However, this type of supervision ignores the fact that the state distribution for the teacher and that of the learner are different [20]. Formally, the distribution of states at test time will not match the distribution at training time, and we therefore cannot expect good long-horizon performance from the learned policy.

In order to overcome this challenge, PLATO uses an adaptive MPC teacher that modifies its actions in order to bring the state distribution in the training data closer to that of the learned policy, while still producing robust trajectories and reacting intelligently to unexpected perturbations that cannot be handled by a partially trained policy. To that end, the teacher generates actions at each time step t from a controller obtained by optimizing the following objective:

$$\pi_\lambda^t(\mathbf{u}|\mathbf{x}_t, \theta) \leftarrow \arg \min_{\pi} J_t(\pi|\mathbf{x}_t) + \lambda D_{\text{KL}}(\pi(\mathbf{u}|\mathbf{x}_t) || \pi_\theta(\mathbf{u}|\mathbf{o}_t)) \quad (1)$$

where λ determines the relative importance of matching the learner π_θ versus optimizing the expected return $J(\cdot)$. Since the teacher uses an MPC algorithm, this objective is reoptimized at each time step to obtain a locally optimal controller for the current state. The only difference from a standard MPC algorithm is the inclusion of the KL-divergence term. The particular MPC algorithm we use is based on iterative LQG (iLQG) [23], using a maximum entropy variant that produces linear-Gaussian stochastic controllers of the form $\pi_\lambda(\mathbf{u}|\mathbf{x}_t) = \mathcal{N}(\mathbf{K}_t \mathbf{x}_t + \mathbf{k}_t, \Sigma_t)$ [11]. The details of this maximum entropy variant of iLQG may be found in prior work [10]. We describe the details of PLATO and its relation to prior methods in Sec. 3.1 and show that PLATO produces a good learned policy in Sec. 4.

3.1 Algorithm Description

Algorithm 1 outlines PLATO. We collect training trajectories by choosing actions \mathbf{u}_t according to an adaptive teacher policy $\pi_\lambda^t(\mathbf{u}|\mathbf{x}_t, \theta)$, which is generated by optimizing the objective in Equation 1 at each time step via iLQG. We then update the learner policy $\pi_\theta(\mathbf{u}|\mathbf{o}_t)$ with supervised learning at the observations \mathbf{o}_t corresponding to the visited states \mathbf{x}_t to minimize the difference between $\pi_\theta(\mathbf{u}|\mathbf{o}_t)$ and the locally optimal policy

$$\pi^*(\mathbf{u}|\mathbf{x}_t) \leftarrow \arg \min_{\pi} J(\pi) \quad (2)$$

which is also obtained via MPC, but without considering the KL-divergence term. This approach ensures the teacher visits states that are similar to those that would be visited by the learner policy π_θ , while still providing supervision from a near-optimal policy. Note that the MPC policy is conditioned on the state of the system \mathbf{x}_t , while the learned policy $\pi_\theta(\mathbf{u}|\mathbf{o}_t)$ is only conditioned on the observations. MPC requires access to at least a rough model of the system dynamics, as well as the system state, in order to robustly choose near-optimal actions. However, by training π_θ on the corresponding observations, instead of the true states, π_θ can learn to process raw sensory inputs without requiring true state observations, making it possible to run the learned policy with only the raw observations at test time. In the rest of this section, we describe the MPC teacher and the supervised learning procedure in detail.

Algorithm 1 PLATO algorithm

- 1: Initialize data $\mathcal{D} \leftarrow \emptyset$
 - 2: **for** $i = 1$ **to** N **do**
 - 3: **for** $t = 1$ **to** T **do**
 - 4: Optimize π_λ^t with respect to Equation (1)
 - 5: Sample $\mathbf{u}_t \sim \pi_\lambda^t(\mathbf{u}|\mathbf{x}_t, \theta)$
 - 6: Optimize π^* with respect to Equation (2)
 - 7: Sample $\mathbf{u}_t^* \sim \pi^*(\mathbf{u}|\mathbf{x}_t)$
 - 8: Append $(\mathbf{o}_t, \mathbf{u}_t^*)$ to the dataset \mathcal{D}
 - 9: State evolves $\mathbf{x}_{t+1} \sim p(\mathbf{x}_{t+1}|\mathbf{x}_t, \mathbf{u}_t)$
 - 10: **end for**
 - 11: Train $\pi_{\theta_{i+1}}$ on \mathcal{D}
 - 12: **end for**
-

Adaptive MPC teacher: The teacher’s policy π_λ^t must take reasonable, robust actions while visiting states that are similar to those that would be seen by the learner policy π_θ . However, we do not know the state distribution of π_θ in advance, since although we have some approximate knowledge of the system dynamics, we do not assume a model of the observation function that produces observations \mathbf{o}_t from states \mathbf{x}_t , making it impossible to simulate the policy π_θ into the future. Instead, we choose the actions at each time step according to an MPC policy π_λ^t that minimizes the expected long-term sum of costs $J_t(\pi_\lambda^t|\mathbf{x}_t)$, but only greedily minimizes the KL-divergence against π_θ at the current time step t , where the observation \mathbf{o}_t is already available, resulting in the objective in Equation 1. Since MPC reoptimizes the local policy at each time step, this method produces a sequence of policies $\pi_\lambda^{1:T}$, each of which is optimized with respect to its long-horizon cost and immediate disagreement with π_θ .

As discussed previously, our iLQG-based MPC algorithm produces linear-Gaussian local controllers $\pi_\lambda^t(\mathbf{u}|\mathbf{x}_t) = \mathcal{N}(\mu_\lambda(\mathbf{x}_t), \Sigma_t)$ where $\mu_\lambda(\mathbf{x}_t) = \mathbf{K}_t\mathbf{x}_t + \mathbf{k}_t$. We will further assume that our learner policy is conditionally Gaussian (but nonlinear), though other parametric distributions are also possible. The policy therefore has the form $\pi_\theta(\mathbf{u}|\mathbf{o}_t) = \mathcal{N}(\mu_\theta(\mathbf{o}_t), \Sigma_{\pi_\theta})$ where $\mu_\theta(\mathbf{o}_t)$ is the output of a nonlinear function, such as a neural network, and Σ_{π_θ} is a learned covariance. Then the MPC objective can be expressed in closed form:

$$\min_{\pi} J_t(\pi|\mathbf{x}_t) + \frac{1}{2}\lambda \left[(\mu_\theta(\mathbf{o}_t) - \mu_\lambda(\mathbf{x}_t))^\top \Sigma_{\pi_\theta}^{-1} (\mu_\theta(\mathbf{o}_t) - \mu_\lambda(\mathbf{x}_t)) + \text{tr}(\Sigma_{\pi_\theta}^{-1}\Sigma_t) + \ln \left(\frac{|\Sigma_{\pi_\theta}|}{|\Sigma_t|} \right) + \text{const} \right]$$

The KL-divergence term in this objective is quadratic in \mathbf{u}_t and linear in the covariance Σ_t , with an entropy maximization term $-\ln|\Sigma_t|$. This is precisely the objective that is optimized by the maximum entropy variant of iLQG [10], and optimization requires us only to expand the cost-to-go J_t to second order, which is a standard procedure in iLQG.

Training the learner’s policy: We want the learner’s policy π_θ to approach the optimal policy $\pi^*(\mathbf{u}|\mathbf{x}_t)$. We can estimate a (locally) optimal policy π^* at each state \mathbf{x}_t with iLQG, simply by repeating the optimization at each time step but excluding the KL-divergence term. During the supervised learning phase, we minimize the KL-divergence between the learner π_θ and the precomputed near-optimal policies π^* at the observations stored in the dataset \mathcal{D} :

$$\theta \leftarrow \arg \min_{\theta} \sum_{(\mathbf{x}_t, \mathbf{o}_t) \in \mathcal{D}} D_{\text{KL}}(\pi_\theta(\mathbf{u}|\mathbf{o}_t) || \pi^*(\mathbf{u}|\mathbf{x}_t)) \quad (3)$$

Since both π_θ and π^* are conditionally Gaussian, the KL-divergence can be expressed in closed-form:

$$\min_{\theta} \frac{1}{2} \sum_{(\mathbf{x}_t, \mathbf{o}_t) \in \mathcal{D}} (\mu^*(\mathbf{x}_t) - \mu_\theta(\mathbf{o}_t))^\top \Sigma_{\pi^*}^{-1} (\mu^*(\mathbf{x}_t) - \mu_\theta(\mathbf{o}_t)) + \text{tr}(\Sigma_{\pi^*}^{-1}\Sigma_{\pi_\theta}) + \ln \left(\frac{|\Sigma_{\pi^*}|}{|\Sigma_{\pi_\theta}|} \right) + \text{const}$$

Ignoring the terms that do not involve the learner policy mean $\mu_\theta(\mathbf{o}_t)$, the objective function can be rewritten in the form of a weighted Euclidean loss:

$$\min_{\theta} \sum_{(\mathbf{x}_t, \mathbf{o}_t) \in \mathcal{D}} \|\mu^*(\mathbf{x}_t) - \mu_\theta(\mathbf{o}_t)\|_{\Sigma_{\pi^*}^{-1/2}}^2$$

This optimization can then be solved using standard regression methods. In our experiments, μ_θ is represented by a neural network, and the above optimization problem corresponds to standard neural network regression, solvable by stochastic gradient descent. The covariance of π_θ can be solved for in closed form, and corresponds to the inverse of the average precisions of π^* at the training points [11].

3.2 Relationship to previous work

The motivation behind PLATO is most similar to the MPC variant of guided policy search (MPC-GPS) [25]. However, PLATO lifts a major limitation of MPC-GPS. MPC-GPS requires the ability to deterministically reset the environment into one of a small set of initial states. In practice, requiring deterministic resets limits the applicability of MPC-GPS and restricts the breadth of data that can be seen at training time. Deterministic episodic resets can be complex, time-consuming, or even impossible in the real world. For example, imagine a robot learning to navigate a human crowd; deterministic resets would require having the crowd walk through the same paths in each episode. Not requiring such resets is a major advantage. Also, even if deterministic resets are feasible, PLATO empirically outperforms MPC-GPS (Section 5).

Formally, PLATO can also be viewed as a generalization of the Dataset Aggregation (DAgger) algorithm [20], which samples trajectories according to the mixture policy $\pi_{\text{MIX}_i} = \beta_i\pi^* + (1-\beta_i)\pi_{\theta_i}$.

approach	teacher policy	supervision policy
supervised learning	π^*	π^*
Dagger	π_{MIX}	π^*
Dagger + coaching	π_{MIX}	π_{COACH}
PLATO	π_λ	π^*

Figure 1: **Overview of teacher-based policy optimization methods:** For PLATO and each prior approach, we list which teacher policy is used for sampling trajectories and which supervision policy is used for generating training actions from the sampled trajectories. Note that the prior methods execute the mixture policy π_{MIX} , which requires running the learned policy π_θ , potentially executing dangerous actions when π_θ has not been fully trained.

The training data is generated from the observations sampled by executing π_{MIX_i} but labelled with actions from π^* . DAgger converges if $\frac{1}{N} \sum_{i=1}^N \beta_i \rightarrow 0$ as $N \rightarrow \infty$. A related extension to DAgger is the method of He et al. [4], which modifies the supervision policy π^* to adapt to the learned policy π_θ . This method, referred to as coaching, labels the training data with a coach policy π_{COACH} that encourages the action training labels to be similar to the actions π_{θ_i} would choose.

Another distinction of PLATO is the use of an adaptive MPC policy $\pi_\lambda^{1:T}$ to select the actions at each time step, rather than the mixture policy π_{MIX} used in the prior methods. As demonstrated in our evaluation, this adaptive MPC policy allows PLATO to robustly avoid catastrophic failure during training, which is particularly important on safety-critical domains such as aerial vehicles. Our experiments also demonstrate that policies trained using PLATO empirically outperform policies trained by either DAgger or coaching. Table 1 summarizes the teacher and supervision policies used by PLATO and prior work.

4 Theoretical Analysis

In this section, we present a proof that the policy π_θ learned by PLATO converges to a policy with bounded cost. This proof extends the result by Ross et al. [20], which only admits mixture policies, to our adaptive MPC policy $\pi_\lambda^{1:T}$. Given a policy π , we use d_π^t to denote the state distribution at time t when executing policy π from time 1 to $t - 1$. We also use $Q_t(\mathbf{x}, \pi, \tilde{\pi})$ to denote the cost of executing π for one time step from initial state \mathbf{x} , and then executing $\tilde{\pi}$ for the remaining $t - 1$ time steps.

When optimizing Equation 1 to obtain the teacher policy π_λ , we choose λ such that $D_{\text{KL}}(\pi_\lambda(\mathbf{u}|\mathbf{x})||\pi_\theta(\mathbf{u}|\mathbf{o})) \leq \epsilon_{\lambda\theta}$ for all state-observation pairs (\mathbf{x}, \mathbf{o}) . We can always guarantee this bound when optimizing Equation 1 because $D_{\text{KL}}(\pi_\lambda(\mathbf{u}|\mathbf{x})||\pi_\theta(\mathbf{u}|\mathbf{o})) \rightarrow 0$ as $\lambda \rightarrow \infty$.

When optimizing the supervised learning objective in Equation 3 to obtain the learner policy π_θ , we assume the supervised learning objective is bounded by a constant $D_{\text{KL}}(\pi_\theta(\mathbf{u}|\mathbf{o})||\pi^*(\mathbf{u}|\mathbf{x})) \leq \epsilon_{\theta^*}$ for all states \mathbf{x} (and corresponding observations \mathbf{o}) in the dataset, which were sampled from the teacher policy distribution d_{π_λ} . Since the policy π_θ is trained with supervised learning precisely on these states $\mathbf{x} \sim d_{\pi_\lambda}$, this corresponds to assuming that the learner policy π_θ attains bounded training error.

We can then prove the following theorem:

Theorem 4.1 *Let $Q_t(\mathbf{x}, \pi_\theta, \pi^*) - Q_t(\mathbf{x}, \pi^*, \pi^*) \leq \delta$ for all $t \in \{1, \dots, T\}$. Then for PLATO, $J(\pi_\theta) \leq J(\pi^*) + \delta\sqrt{\epsilon_{\theta^*}}O(T) + O(1)$*

The proof, presented in Appendix B, consists of first showing that the difference in the state distributions of the teacher and learner is bounded if the KL-divergence of their policies is bounded (see Appendix A), and then using this fact to derive an upper bound on the expected cost of the learned policy π_θ under its own state distribution. Since we can make $\epsilon_{\lambda\theta}$ arbitrarily low by choosing the value λ , we choose $\epsilon_{\lambda\theta} = O(\frac{1}{T^2})$ to obtain the result in Theorem 4.1.

5 Experiments

We evaluate PLATO on a series of simulated quadrotor navigation tasks. MPC is a standard choice for quadrotor control because approximate models are typically known in advance from standard rigid body physics and the vehicle specifications. However, effective use of MPC requires explicit state estimation and can be computationally intensive. It is therefore very appealing to be able to train an entirely feedforward, reactive policy to control a quadrotor performing navigation in obstacle-rich environments, directly in response to raw sensor inputs. During training, the vehicle might be placed in a known, instrumented training environment to collect data using MPC, while at test time, the

learned feedforward policy could control the aircraft directly from raw observations. This makes simulated quadrotor navigation an ideal domain in which to compare PLATO to prior work.

Prior Methods and Baselines: We compare PLATO to four methods. The first method is DAgger, which, as discussed in Section 3.2, executes a mixture of the learned policy and teacher policy, which in this case is MPC (without a KL-divergence term). DAgger has previously been used for learning quadrotor control policies from human demonstrations [21]. While DAgger carries the same convergence guarantees as PLATO, successful use of DAgger requires the learned policy to be executed at training time, before the policy has converged to a near-optimal behavior. The second method is the coaching algorithm of He et al. [4] which, like DAgger, executes a mixture of the learned and teacher policies, but supervises the learner using the adapted policy. In these experiments, we chose the coaching policy π_{COACH} to be the teacher policy π_{λ} from PLATO. For both DAgger and coaching, we must choose the mixing parameter β_i at each iteration i . Since the performance of these algorithms is quite sensitive to the schedule of the β_i parameter, we include four schedules for comparison: three linear schedules that interpolate β_i from 1 at the first iteration to 0 at the last iteration (“linear full”), the halfway iteration (“linear half”), and the quarter-way iteration (“linear quarter”), as well as the more standard “1-0” schedule that sets $\beta_i = 1[i = 1]$. The third method is MPC-GPS [25], which unlike PLATO, DAgger and coaching requires deterministic resets during training. In addition to these prior methods, we also compare our approach to a standard supervised learning baseline, which always executes the MPC policy without any adaptation.

Policy Representation: For all of the methods, we represent π_{θ} as a conditional Gaussian policy, with a constant covariance and a mean given by a neural network function of the observation \mathbf{o}_t . The neural network architecture and optimization method are described in Appendix E.

Experimental Domains: The comparisons are conducted on two test environments: a winding canyon with randomized turns, and a dense forest of cylindrical trees with randomized positions. An example environment is shown in Figure 2. Further details are provided in Appendix C.

The dynamical system is a quadrotor with dynamics described by [14]. The state of the vehicle $\mathbf{x} \in \mathbb{R}^{13}$ consists of the position and orientation, as well as their time derivatives, and the control $\mathbf{u} \in \mathbb{R}^4$ consists of motor velocities. The observations \mathbf{o} consist of orientation, linear velocity, angular velocity and either (i) a set of 30 equally spaced 1-d laser depth scanners arranged in 180 degree fan in front of the vehicle ($\mathbf{o} \in \mathbb{R}^{40}$) or (ii) a 5×20 grayscale camera image ($\mathbf{o} \in \mathbb{R}^{110}$). Learning neural network policies with these observations forces the policies to perform both perception and control, since success on each of the domains requires avoiding obstacles using only raw sensory input.

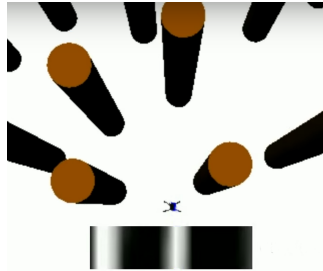


Figure 2: Quadrotor in forest with camera

The cost function for the MPC teacher encourages the quadrotor to fly at a specific linear velocity and orientation while minimizing control effort and avoiding collisions. The desired velocity and direction are either kept constant or, in the case of policies with commanded velocity discussed in a following section, varied at random intervals to simulate user commands. A more formal definition of the cost function is provided in Appendix D.

Performance of Learned Policies: In Figures 3a, 3b, 3d, and 3e, we present the mean time to failure (MTTF) of the learned policy π_{θ} on the canyon and forest environments using the laser or camera sensors. The graphs show the MTTF of each policy at each iteration of the learning process, averaged over 10 training runs of each method with 20 repetitions each. Failure occurs when the quadrotor crashes into an obstacle, with the maximum flight time for each domain listed on the graphs. The results indicate that the PLATO algorithm is able to learn effective policies faster, and converges to a solution that is better than or comparable to the baseline methods. For some choices of β schedule and supervision scheme, some DAgger variants achieve similar final MTTFs, but always at a slower rate and, as discussed next, with significantly more training crashes.

Robustness During Training: In Figures 3a, 3b, 3d, and 3e, we show the number of crashes experienced during training at each iteration. PLATO on average experiences less than one crash per iteration, comparable in performance to the baseline MPC method (supervised learning), indicating that mimicking the learner with a KL-divergence penalty does not substantially degrade the robustness

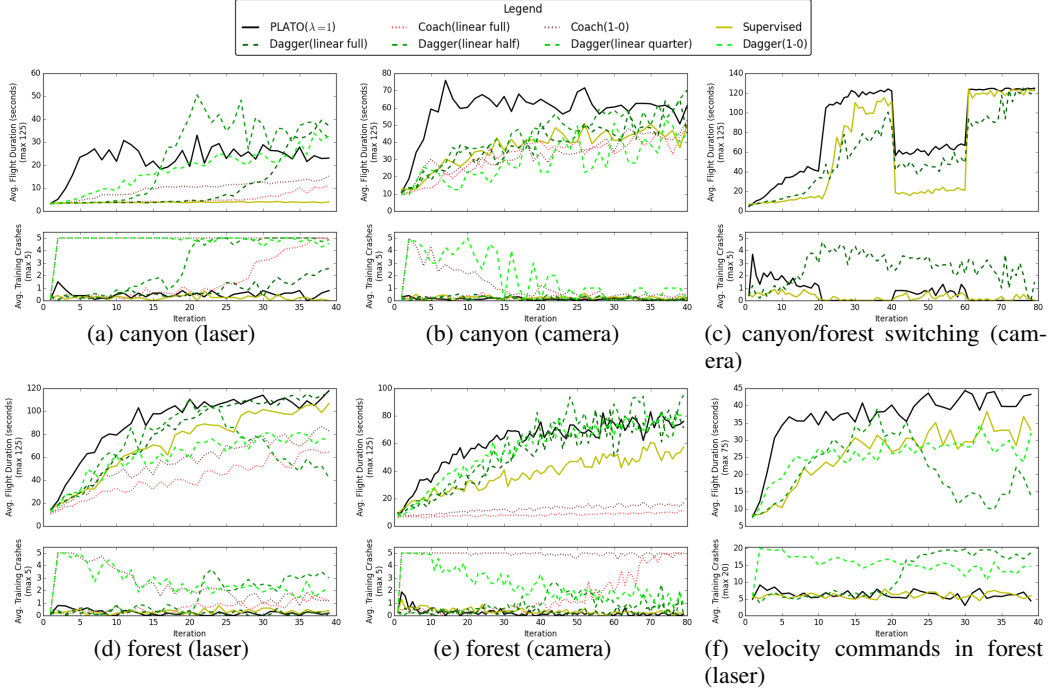


Figure 3: **Experiments:** We compare PLATO to baseline methods in a winding canyon, a dense forest, and an alternating canyon/forest. For each scenario and learning method, we trained 10 different policies using different random seeds. Then for each policy, we evaluated the neural network policy trained at each iteration by flying through the scenario 20 times. Therefore each datapoint corresponds to 200 samples.

of MPC. In contrast, both DAGger and coaching begin to experience a substantial number of failures when the mixing constant β drops. By carefully selecting the schedule for β , the number of crashes can be reduced.

However, even with a carefully chosen schedule, the prior methods are vulnerable to non-stationary training environments, as illustrated in Figure 3c. In this experiment, the vehicle switches from the canyon to the forest halfway through training, and then switches back to the forest. PLATO still experienced on average less than one crash per episode in this mode, but the prior methods that directly execute π_θ during training could not cope with this condition, since a policy trained only on the canyon cannot succeed on the forest without additional training. While this example might appear pathological, it is in fact a plausible training setup for a real quadrotor exploring a varied environment, such as different floors of a building. If the walls on one floor are painted, e.g., a different color than the rest, the learned policy could easily experience a catastrophic failure when entering the floor for the first time, even if it was consistently successful on preceding floors.

Sensitivity to KL-Divergence Weight: Figure 4 compares different settings of the λ parameter. Recall that λ determines the degree to which MPC prioritizes following the learner π_θ versus performing the desired task. For very small values of λ , the performance of PLATO approaches standard supervised learning, while for very large values, it is similar to DAGger. However, the results suggest that a relatively broad range of λ values produces successful policies.

Policies with Velocity Commands: Figure 3f shows the performance of PLATO when learning policies that take an additional input in the form of a commanded velocity, to simulate high-level user control. These policies are useful because instead of training multiple policies for different target velocities, we can train one generalizable policy. This input modifies the cost function used by MPC, producing command-aware supervision. During training, the commands vary in the range of ± 1 m/s sideways and 1 to 2.5 m/s forward. At test time, we sample velocity commands uniformly at random; the velocity commands

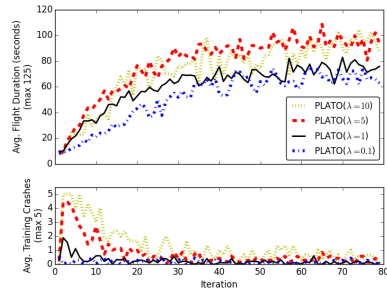


Figure 4: Effect of KL-divergence weight λ

are re-sampled whenever the quadrotor reaches the current sampled velocity. The results indicate that PLATO can successfully learn such policies, outperforming prior methods and again minimizing the number of crashes during training.

Comparison with MPC-GPS: MPC-GPS [25] cannot directly be evaluated on the domains described above, because training must occur in episodes with deterministic resets (see Section 3.2). We constructed a fixed-length episodic variant of the forest task where MPC-GPS was allowed to use deterministic resets. Besides not requiring an episodic formulation or deterministic resets, the comparison in Figure 5 shows that PLATO substantially outperforms the policy learned by MPC-GPS in terms of MTTF.

Supplementary material, including a video, can be viewed online ¹.

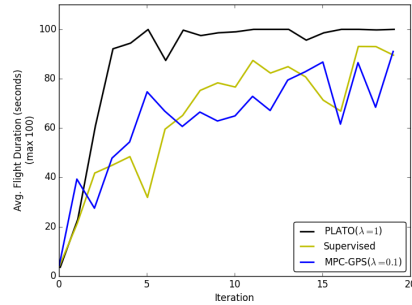


Figure 5: Comparison with MPC-GPS

6 Discussion

In this paper, we presented PLATO, an algorithm for learning complex, high-dimensional policies that combine perception and control into a single expressive function approximator, such as a deep neural network. PLATO uses a trajectory optimization teacher to provide supervision to a standard supervised learning algorithm, allowing for a simple and data-efficient learning method. The teacher adapts to the behavior of the neural network policy to ensure that the distribution over states and observations is sufficiently close to the learned policy, allowing for a bound on the long-term performance of the learned policy. Our empirical evaluation, conducted on a set of challenging simulated quadrotor domains, demonstrates that PLATO outperforms a number of previous methods, both in terms of the robustness and effectiveness of the final policy, and in terms of the safety of the training procedure.

PLATO has two key advantages that make it well-suited for learning control policies for real-world robotic systems. First, since the learned neural network policy does not need to be executed at training time, the method benefits from the robustness of model-predictive control (MPC), minimizing catastrophic failures at training time. This is particularly important when the distribution over training states and observations is non-stationary, as in the canyon/forest switching scenario. Here, methods that execute the learned policy, such as DAGger, can suffer a catastrophic failure when the agent encounters observations that are too different from those seen previously. Mitigating these issues typically requires hand-designed safety mechanisms, while PLATO automatically switches to a more off-policy behavior.

The second advantage of PLATO is that the learned policy can use a different set of observations than MPC. Effective use of MPC requires observing or inferring the full state of the system, which might be accomplished, for instance, by instrumenting the environment with motion capture, or using a known map with relocalization [24]. The policy, however, can be trained directly on raw input from onboard sensors, forcing it to perform both perception and control. Once trained, such a policy can be used in uninstrumented natural environments.

PLATO shares these benefits with recently developed guided policy search algorithms [25]. However, in contrast with guided policy search, PLATO does not require a carefully designed episodic environment and deterministic resets. In fact, the policy can be learned equally well for infinite horizon tasks without episodic structure or reset mechanisms, making it more data-efficient and practical, for example, for learning navigation policies in varied environments.

One of the most appealing prospects of learning expressive neural network policies with an automated MPC teacher is the possibility of acquiring real-world policies that directly use rich sensory inputs, such as camera images, depth sensors, and other inputs that are difficult to process with standard model-based techniques. Because of this, one very interesting avenue for future work is to apply PLATO on real physical platforms, especially ones equipped with novel and unusual sensors.

References

- [1] Chen, C., Seff, A., Kornhauser, A., and Xiao, J. Deepdriving: learning affordance for direct perception in autonomous driving. In *IEEE International Conference on Computer Vision (ICCV)*, 2015.

¹sites.google.com/site/platopolicy

- [2] Deisenroth, M. P., Neumann, G., and Peters, J. A survey on policy search for robotics. In *Foundations and Trends in Robotics*, 2011.
- [3] Giusti, A., Guzzi, J., Ciresan, D. C., He, F., Rodriguez, J. P., Fontana, F., Faessler, M., Forster, C., Schmidhuber, J., Caro, G., Scaramuzza, D., and Gambardella, L. A machine learning approach to visual perception of forest trails for mobile robots. In *IEEE Robotics and Automation Letters*, 2016.
- [4] He, H., Eisner, J., and Daume, H. Imitation learning by coaching. In *Advances in Neural Information Processing Systems (NIPS)*, 2012.
- [5] Heess, N., Wayne, G., Silver, D., Lillicrap, T., Tassa, Y., and Erez, T. Learning continuous control policies by stochastic value gradients. In *Advances in Neural Information Processing Systems (NIPS)*, 2015.
- [6] Jia, Y., Shelhamer, E., Donahue, J., Karayev, S., Long, J., Girshick, R., Guadarrama, S., and Darrell, T. Caffe: Convolutional architecture for fast feature embedding. *arXiv preprint arXiv:1408.5093*, 2014.
- [7] Kingma, D.P. and Ba, J. Adam: A method for stochastic optimization. In *International Conference on Learning Representations (ICLR)*, 2015.
- [8] LeCun, Yann, Bengio, Yoshua, and Hinton, Geoffrey. Deep learning. *Nature*, 521(7553):436–444, 2015.
- [9] Levin, D. A., Peres Y. and Wilmer, E. L. *Markov chains and mixing times*. American Mathematical Soc., 2009.
- [10] Levine, S. and Abbeel, P. Learning neural network policies with guided policy search under unknown dynamics. In *Advances in Neural Information Processing Systems (NIPS)*, 2014.
- [11] Levine, S. and Koltun, V. Guided policy search. In *International Conference on Machine Learning (ICML)*, 2013.
- [12] Levine, S., Finn, C., Darrell, T., and Abbeel, P. End-to-end training of deep visuomotor policies. *arXiv preprint arXiv:1504.00702*, 2015.
- [13] Lillicrap, T. P., Hunt, J. J., Pritzel, A., Heess, N., Erez, T., Tassa, Y., Silver, D., and Wierstra, D. Continuous control with deep reinforcement learning. In *arXiv:1411.0247*, 2015.
- [14] Martin, P. and Salaun, E. The true role of accelerometer feedback in quadrotor control. In *Proc. IEEE Int. Conf. Robotics and Automation (ICRA)*, 2010.
- [15] Mayne, D.Q., Seron, M. M., and Rakovic, S. V. Robust model predictive control of constrained linear systems with bounded disturbances. In *Automatica*, 2005.
- [16] Mnih, V., Kavukcuoglu, K., Silver, D., Graves, A., Antonoglou, I., Wierstra, D., and M., Riedmiller. Playing atari with deep reinforcement learning. In *Workshop on Deep Learning, Advances in Neural Information Processing Systems (NIPS)*, 2013.
- [17] Nair, V. and Hinton, G. Rectified linear units improve restricted boltzmann machines. In *International Conference on Machine Learning (ICML)*, 2010.
- [18] Nguyen, X., Wainwright, M. J., and Jordan, M. I. Divergences, surrogate loss functions and experimental design. In *Advances in Neural Information Processing Systems (NIPS)*, 2005.
- [19] Pollard, D. Asymptopia: an exposition of statistical asymptotic theory. 2000. URL <http://www.stat.yale.edu/~pollard/Books/Asymptopia/>.
- [20] Ross, S., Gordon G. J. and Bagnell, J. A. A reduction of imitation learning and structured prediction to no-regret online learning. In *Proceedings of the 14th International Conference on Artificial Intelligence and Statistics (AISTATS)*, 2011.
- [21] Ross, S., Melik-Barkhudarov N. Shankar K. S. Wendel A. Dey D. Bagnell J. A. and Hebert, M. Learning monocular reactive uav control in cluttered natural environments. In *Proceedings of the IEEE International Conference on Robotics and Automation (ICRA)*, 2013.
- [22] Schulman, J., Levine, S., Moritz, P., Jordan, M. I., and Abbeel, P. Trust region policy optimization. In *Proceedings of the International Conference on Machine Learning (ICML)*, 2015.
- [23] Todorov, E. and Li, W. A generalized iterative LQG method for locally-optimal feedback control of constrained nonlinear stochastic systems. In *American Control Conference*, 2005.
- [24] Williams, B., Klein, G., and Reid, I. Real-time slam relocalisation. In *International Conference on Computer Vision (ICCV)*, 2007.
- [25] Zhang, T., Kahn, G., Levine, S., and Abbeel, P. Learning deep control policies for autonomous aerial vehicles with mpc-guided policy search. In *Proc. IEEE Int. Conf. Robotics and Automation (ICRA)*, 2016.

A Proof of State Distribution Bound

Given a policy π , we denote d_π^t as the state distribution at time t when executing policy π from time 1 to $t - 1$.

We will first re-derive the following state distribution bound:

Lemma A.1 [20] $\|d_{\pi_{\text{MIX}_i}}^t - d_{\pi_{\theta_i}}^t\|_1 \leq 2t\beta_i$

Proof. The mixture policy is defined as $\pi_{\text{MIX}_i} = \beta_i\pi^* + (1 - \beta_i)\pi_{\theta_i}$. Define d^t as the distribution of states over t steps conditioned on π_{MIX_i} choosing π^* at least once over t steps. Since π_{MIX_i} always executes π_{θ_i} over t steps with probability $(1 - \beta_i)^t$ we have $d_{\pi_{\text{MIX}_i}} = (1 - \beta_i)^t d_{\pi_{\theta_i}}^t + (1 - (1 - \beta_i)^t) d^t$. Thus

$$\begin{aligned} \|d_{\pi_{\text{MIX}_i}}^t - d_{\pi_{\theta_i}}^t\|_1 &= (1 - (1 - \beta_i)^t) \|d^t - d_{\pi_{\theta_i}}^t\|_1 \\ &\leq 2(1 - (1 - \beta_i)^t) \\ &\leq 2t\beta_i \end{aligned}$$

The last inequality follows from the fact that $(1 - \beta)^t \geq 1 - \beta t$ for $\beta \in [0, 1]$. \square

We will now adapt Lemma A.1 to the case where π_{MIX} is not necessarily a mixture involving π_θ , but instead consists of two arbitrary policies π and $\tilde{\pi}$ and the maximum KL-divergence between the two policies. Define $D_{\text{KL}}^{\text{max}}(\pi_{\text{MIX}}, \pi_\theta) = \max_{\mathbf{x}} D_{\text{KL}}(\pi_{\text{MIX}}(\cdot|\mathbf{x})||\pi_\theta(\cdot|\mathbf{x}))$, then:

Lemma A.2 $\|d_\pi^t - d_{\tilde{\pi}}^t\|_1 \leq 2t\sqrt{D_{\text{KL}}^{\text{max}}(\pi, \tilde{\pi})}$

Proof. Similar to [22], the main idea is to couple the two policies so that they choose the same action with probability $1 - \beta$.

Lemma A.3 [9] *Suppose p_X and p_Y are distributions with total variation divergence $D_{\text{TV}}(p_X||p_Y) = \beta$. Then there exists a joint distribution (X, Y) whose marginals p_X, p_Y , for which $X = Y$ is with probability $1 - \beta$.*

This joint distribution is constructed as follows:

- (i) With probability β , we sample X from $\max(p_X - p_Y, 0)/\beta$ and sample Y from $\max(p_Y - p_X, 0)/\beta$
- (ii) With probability $1 - \beta$, we sample $X = Y$ from $\min(p_X, p_Y)/(1 - \beta)$

The sampling distribution in (i) places all the probability mass in regions where $X \neq Y$ and (ii) is chosen such that the joint is a valid distribution.

Let $\mathbf{u}_{\pi_{\text{MIX}}}, \mathbf{u}_{\pi_\theta}$ be random variables which represent the actions chosen by policies π_{MIX} and π_θ . Let $\beta = D_{\text{TV}}^{\text{max}}(\pi_{\text{MIX}}(\cdot|\mathbf{x})||\pi_\theta(\cdot|\mathbf{x}))$. By Lemma A.3, we can define $\mathbf{u}_{\pi_{\text{MIX}}}, \mathbf{u}_{\pi_\theta}$ on a common probability space so that

$$p(\mathbf{u}_{\pi_{\text{MIX}}} \neq \mathbf{u}_{\pi_\theta}) = D_{\text{TV}}(\pi_{\text{MIX}}(\cdot|\mathbf{x})||\pi_\theta(\cdot|\mathbf{x})) \leq \beta$$

We note the following relationship between total variation divergence and the KL divergence [19]: $D_{\text{TV}}(p||q)^2 \leq D_{\text{KL}}(p||q)$. Substituting for β in Lemma A.1:

$$\begin{aligned} \|d_{\pi_{\text{MIX}}}^t - d_{\pi_\theta}^t\|_1 &\leq 2t\beta \\ &= 2tD_{\text{TV}}^{\text{max}}(\pi_{\text{MIX}}, \pi_\theta) \\ &\leq 2t\sqrt{D_{\text{KL}}^{\text{max}}(\pi_{\text{MIX}}, \pi_\theta)} \end{aligned}$$

Note that the last equation makes no assumption about π_{MIX} being a mixture involving π_θ . Therefore for any two policies π and $\tilde{\pi}$:

$$\|d_\pi^t - d_{\tilde{\pi}}^t\|_1 \leq 2t\sqrt{D_{\text{KL}}^{\text{max}}(\pi, \tilde{\pi})}$$

\square

B Proof of PLATO Convergence

B.1 Preliminaries

Given a policy π , we denote d_π^t as the state distribution at time t when executing policy π from time 1 to $t - 1$.

Define the cost function $c(\mathbf{x}_t, \mathbf{u}_t)$ as a function of state \mathbf{x}_t and control \mathbf{u}_t , with $c(\mathbf{x}_t, \mathbf{u}_t) \in [0, 1]$ without loss of generality. We wish to learn a policy $\pi_\theta(\mathbf{u}|\mathbf{o}_t)$ that minimizes the total expected cost over time horizon T :

$$J(\pi) = \sum_{t=1}^T \mathbb{E}_{\mathbf{x}_t \sim d_\pi^t} [\mathbb{E}_{\mathbf{u}_t \sim \pi_\theta(\mathbf{u}|\mathbf{o}_t)} [c(\mathbf{x}_t, \mathbf{u}_t) | \mathbf{x}_t]]$$

Let $J_t(\pi, \tilde{\pi})$ denote the expected cost of executing π for t time steps, and then executing $\tilde{\pi}$ for the remaining $T - t$ time steps.

Let $Q_t(\mathbf{x}, \pi, \tilde{\pi})$ denote the cost of executing π for one time step starting from initial state \mathbf{x} , and then executing $\tilde{\pi}$ for the remaining $t - 1$ time steps. We assume the cost-to-go difference between the learned policy and the optimal policy is bounded: $Q_t(\mathbf{x}, \pi_\theta, \pi^*) - Q_t(\mathbf{x}, \pi^*, \pi^*) \leq \delta$.

When optimizing Equation 1 to obtain the teacher policy π_λ , we choose λ such that $D_{\text{KL}}(\pi_\lambda(\mathbf{u}|\mathbf{x}) || \pi_\theta(\mathbf{u}|\mathbf{o})) \leq \epsilon_{\lambda\theta}$ for all state-observation pairs (\mathbf{x}, \mathbf{o}) . We can always guarantee this bound when optimizing Equation 1 because $D_{\text{KL}}(\pi_\lambda(\mathbf{u}|\mathbf{x}) || \pi_\theta(\mathbf{u}|\mathbf{o})) \rightarrow 0$ as $\lambda \rightarrow \infty$.

When optimizing the supervised learning objective in Equation 3 to obtain the learner policy π_θ , we assume the supervised learning objective function error is bounded by a constant $D_{\text{KL}}(\pi_\theta(\mathbf{u}|\mathbf{o}) || \pi^*(\mathbf{u}|\mathbf{x})) \leq \epsilon_{\theta^*}$ for all states \mathbf{x} (and corresponding observations \mathbf{o}) in the dataset, which were sampled from the teacher policy distribution d_{π_λ} . Since the policy π_θ is trained with supervised learning precisely on these states $\mathbf{x} \sim d_{\pi_\lambda}$, this bound ϵ_{θ^*} corresponds to assuming that the learner policy π_θ attains bounded training error.

Let $l(\mathbf{x}, \pi_\theta, \pi^*)$ denote the expected 0-1 loss of π_θ with respect to π^* in state \mathbf{x} : $\mathbb{E}_{\mathbf{u}_\theta \sim \pi_\theta(\mathbf{u}|\mathbf{o}), \mathbf{u}^* \sim \pi^*(\mathbf{u}|\mathbf{x})} [\mathbf{1}[\mathbf{u}_\theta \neq \mathbf{u}^*]]$. We note that the total variation divergence is an upper bound on the 0-1 loss [18] and the KL-divergence is an upper bound on the total variation divergence [19]. Therefore for all states $\mathbf{x} \sim d_{\pi_\lambda}$ in the dataset used for supervised learning, the 0-1 loss can be upper bounded:

$$\begin{aligned} l(\mathbf{x}, \pi_\theta, \pi^*) &= \mathbb{E}_{\mathbf{u}_\theta \sim \pi_\theta(\mathbf{u}|\mathbf{o}), \mathbf{u}^* \sim \pi^*(\mathbf{u}|\mathbf{x})} [\mathbf{1}[\mathbf{u}_\theta \neq \mathbf{u}^*]] \\ &\leq D_{\text{TV}}(\pi_\theta(\mathbf{u}|\mathbf{o}) || \pi^*(\mathbf{u}|\mathbf{x})) \\ &\leq \sqrt{D_{\text{KL}}(\pi_\theta(\mathbf{u}|\mathbf{o}) || \pi^*(\mathbf{u}|\mathbf{x}))} \\ &\leq \sqrt{\epsilon_{\theta^*}} \end{aligned}$$

We also note the state distribution bound $\|d_\pi^t - d_{\tilde{\pi}}^t\|_1 \leq 2t\sqrt{D_{\text{KL}}^{\max}(\pi, \tilde{\pi})}$ proven in Appendix A. This lemma implies that for an arbitrary function $f(\mathbf{x})$, $E_{\mathbf{x} \sim d_\pi^t} [f(\mathbf{x})] \leq E_{\mathbf{x} \sim d_{\tilde{\pi}}^t} [f(\mathbf{x})] + 2f^{\max} t \sqrt{D_{\text{KL}}^{\max}(\pi, \tilde{\pi})}$

B.2 Proof

We will now prove Theorem 4.1:

$$\begin{aligned}
& J(\pi_\theta) \\
&= J(\pi^*) + \sum_{t=0}^{T-1} J_{t+1}(\pi_\theta, \pi^*) - J_t(\pi_\theta, \pi^*) \\
&= J(\pi^*) + \sum_{t=1}^T \mathbb{E}_{\mathbf{x} \sim d_{\pi_\theta}^t} [Q_t(\mathbf{x}, \pi_\theta, \pi^*) - Q_t(\mathbf{x}, \pi^*, \pi^*)] \\
&\leq J(\pi^*) + \delta \sum_{t=1}^T \mathbb{E}_{\mathbf{x} \sim d_{\pi_\theta}^t} [l(\mathbf{x}, \pi_\theta, \pi^*)] \tag{4a}
\end{aligned}$$

$$\leq J(\pi^*) + \delta \sum_{t=1}^T \mathbb{E}_{\mathbf{x} \sim d_{\pi_\lambda}^t} [l(\mathbf{x}, \pi_\theta, \pi^*)] + 2l^{\max} t \sqrt{\epsilon_{\lambda\theta}} \tag{4b}$$

$$\begin{aligned}
&\leq J(\pi^*) + \delta \sum_{t=1}^T \sqrt{\epsilon_{\theta^*}} + 2t \sqrt{\epsilon_{\theta^*}} \sqrt{\epsilon_{\lambda\theta}} \tag{4c} \\
&= J(\pi^*) + \delta T \sqrt{\epsilon_{\theta^*}} + \delta T(T+1) \sqrt{\epsilon_{\theta^*}} \sqrt{\epsilon_{\lambda\theta}}
\end{aligned}$$

Equation 4a follows from the fact that the expected 0-1 loss of π_θ with respect to π^* is the probability that π_θ and π^* pick different actions in \mathbf{x} ; when they choose different actions, the cost-to-go increases by $\leq \delta$.

Equation 4b follows from the state distribution bound proven in Appendix A.

Equation 4c follows from the upper bound on the 0-1 loss.

Although we do not get to choose ϵ_{θ^*} because that is a property of the supervised learning algorithm and the data, we are able to choose $\epsilon_{\lambda\theta}$ by varying parameter λ . If we choose λ such that $\epsilon_{\lambda\theta} = O(\frac{1}{T^2})$, then

$$J(\pi_\theta) \leq J(\pi^*) + \delta \sqrt{\epsilon_{\theta^*}} O(T) + O(1)$$

□

As with DAgger, in the worst case $\delta = O(T)$. However, in many cases $\delta = O(1)$ or is sub-linear in T , for instance if π^* is able to quickly recover from mistakes made by π_θ .

We also note that this bound is the same as the bound obtained by DAgger, but without actually needing to directly execute π_θ at training time.

Figure 6 illustrates how the teacher policy π_λ and learner policy π_θ change while running the PLATO algorithm.

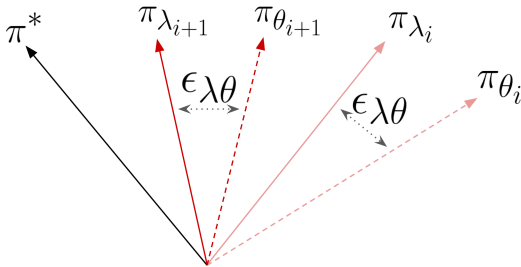


Figure 6: PLATO diagram illustrating the policy updates. Let all policies be represented as vectors in a vector space. Consider the PLATO algorithm at iteration i with the current learned policy π_{θ_i} . The learner policy π_{λ_i} is then optimized to be within $\epsilon_{\lambda\theta}$ “distance” of π_{θ_i} ; however π_{λ_i} is closer to π^* than π_{θ_i} due to the formulation of the optimization in Equation 1. We sample trajectories with π_{λ_i} and label the actions using π^* . $\pi_{\theta_{i+1}}$ is then trained, which is closer to π^* than the previous iteration’s learned policy π_{θ_i} . The PLATO algorithm continues until convergence.

C Domain Details

The quadrotor has a radius of 0.42m.

The canyon scenario in Fig. 3b is composed of 0.5m long segments that randomly change direction by ± 1.0 radians with a maximum angle of $\frac{\pi}{4}$ radians. The target velocity was 6.0 m/s.

The forest scenario in Fig. 3e and 4 is composed of cylinders of radius 0.5m and height 40m with a minimum spacing of 2.5m and an average spacing of 2.75m between cylinders. The target velocity was 2.0 m/s.

The scenario in Fig. 3c alternates between a canyon scenario and forest scenario every 20 iterations. The canyon scenario is the same as above. The forest scenario is the same as above except with a minimum spacing of 3.0m and an average spacing of 3.25m between cylinders. The target velocity was 4.0 m/s.

D Teacher Cost Function

The teacher cost function was

$$\begin{aligned} L(\mathbf{x}, \mathbf{u}) = & 10^3 \|\mathbf{x}_{\text{LINVEL}} - \mathbf{x}_{\text{LINVEL}}^*\|_2^2 + \\ & 10^3 \|\mathbf{x}_{\text{HEIGHT}} - \mathbf{x}_{\text{HEIGHT}}^*\|_2^2 + \\ & 10^4 \|\mathbf{x}_{\text{QUAT}} - \mathbf{x}_{\text{QUAT}}^*\|_2^2 + \\ & 250 \|\mathbf{x}_{\text{ANGVEL}}\|_2^2 + \\ & 5^{-3} \|\mathbf{u} - \mathbf{u}_{\text{HOVER}}\|_2^2 + \\ & 10^3 \max(d_{\text{SAFE}} - \text{signed-distance}(\mathbf{x}), 0) \end{aligned}$$

where $\mathbf{x}_{\text{LINVEL}}, \mathbf{x}_{\text{HEIGHT}}, \mathbf{x}_{\text{QUAT}}, \mathbf{x}_{\text{ANGVEL}}$ are the linear velocity, height, orientation, and angular velocity of the state \mathbf{x} , respectively; $\mathbf{x}_{\text{LINVEL}}^*, \mathbf{x}_{\text{HEIGHT}}^*, \mathbf{x}_{\text{QUAT}}^*$ are the target linear velocity, height, and orientation, respectively; and $\mathbf{u}_{\text{HOVER}}$ is the rotor velocity when the quadrotor is hovering. The final term is a hinge loss on the distance of the quadrotor to the nearest obstacle; there is no penalty if the nearest obstacle is further than d_{SAFE} .

E Neural Network Details

We used Caffe [6] for our neural network. The network has two hidden layers each of size 40. Each layer is connected by an inner product, and for the hidden layers followed by a Rectified Linear Unit (ReLU) [17]. We used the ADAM [7] solver with batch size 50 and 20000 iterations to optimize the neural network policy π_θ . We used Xavier initialization for the weights on the first iteration; subsequent iterations had initial weights based on those from the previous iteration. The loss function was a weighted euclidean loss as stated in Section 3.1.